Simulating Multi-scale, Granular Materials and Their Transitions with a Hybrid Euler-Lagrange Solver

Yang Gao, Shuai Li, Aimin Hao, and Hong Qin,*Member, IEEE,*

Abstract—Multi-scale granular materials, such as powdered materials and mudslides, are pretty common in nature. Modeling such materials and their phase transitions remains challenging since this task involves the delicate representations of various ranges of particles with multiple scales that cause their property variations among liquid, granular solid (i.e., particles), and smoke-like materials. To effectively animate the complicated yet intriguing natural phenomena involving multi-scale granular materials and their phase transitions in graphics with high fidelity, this paper advocates a hybrid Euler-Lagrange solver to handle the behaviors of involved discontinuous fluid-like materials faithfully. At the algorithmic level, we present a unified framework that tightly couples the affine particle-in-cell (APIC) solver with density field to achieve the transformation spanning across granular particles, dust cloud, powders, and their natural mixtures. For example, a part of the granular particles could be transformed into dust cloud while interacting with air and being represented by density field. Meanwhile, the velocity decrease of the involved materials could also result in the transit from the density-field-driven dust to powder particles. Besides, to further enhance our modeling and simulation power to broaden the range of multi-scale materials, we introduce a moisture property for granular particles to control the transitions between particles and viscous liquid. At the geometric level, we devise an additional surface-tracking procedure to simulate the viscous liquid phase. We can arrive at delicate viscous behaviors by controlling the corresponding yield conditions. Through various experiments with the different scenes design being conducted in our unified framework, we can validate the mixed multi-scale materials' mutual transformation processes. Our unified framework furnished with a hybrid solver can significantly enhance the modeling flexibility and the animation potential of the particle-grid hybrid materials in graphics.

Index Terms—Multi-scale Materials; Granular Particles; Density-field-based Dust Cloud; Viscous Liquid; APIC.

1 Introduction

The multi-scale, granular materials are common in our daily lives, which involve various kinds of phases with different scales such as liquid, granular particles, and dust cloud. Such materials move like liquid, but have more complicated behaviors and involve the delicate components of various ranges of particles with multiple scales, taking on different forms while moving. Modeling all types of materials with their dynamic transitions within a unified framework is challenging. For most existing researches, granular or powdered granular material is usually simulated as a single kind of particle with constant size. The classical simulation methods include smoothed particle hydrodynamics (SPH) [1], [2], position-based dynamics (PBD) [3], fluid implicit particle (FLIP) / particle in cell (PIC) [4], [5], material point method (MPM) [6], [7], [8], etc. At the geometric modeling level, existing works always take the discrete particles as the same substance with the same size [9], [4], [10]. They have difficulties achieving realistic effects like dust dispersal or solid-liquid mixtures. At the pure dynamics-driven simulation level, researchers can classify such multi-scale materials according to their physical properties to model the mixtures and movements [10], [11], [12]. However, they are hard to handle the complicated transitions among multi-scale particles.

In reality, granular materials always contain various particles of different scales, which exhibit different properties while moving. Of which, fine-grained particles may not follow other coarse particles during throwing, due to the small size and lightweight, fine-grained dust is more affected by air friction to float as dust cloud, and then gradually settle on the floor [13]. Meanwhile, when a large number of particles are gathered together, they may appear to be highly similar to liquid flowing. Gao [14] and his colleagues simulated powder materials by combining the Lagrange model and the density field, which is the first attempt to model and simulate powdered material with different materials, but they did not consider the fluid-like properties that may exhibit in most cases. Multi-scale granular materials are similar to particle-based materials, and in some violent moving scenes, such as mudslide, the discontinuous materials may contain viscous liquid, powdered particles, and dust cloud simultaneously, which is severely difficult to model in a united hybrid framework.

This paper aims to tackle this challenging phenomenon and simulate multi-scale granular materials' vivid and sufficient behaviors, including particles phase, density field,

- *Y. Gao, S. Li and A. Hao are with State Key Laboratory of Virtual Reality Technology and Systems, Beijing Advanced Innovation Center for Biomedical Engineering, Beihang University, Beijing, China. They are also with the Research Unit of Virtual Human and Virtual Surgery (2019RU004), Chinese Academy of Medical Sciences, China.*
  S. Li and A. Hao are with Peng Cheng Laboratory, Shenzhen, China.
- *H. Qin is with Department of Computer Science, Stony Brook University (SUNY at Stony Brook), New York 11733, USA.*

qin@cs.stonybrook.edu

liquid phase, and their natural mixtures. We consider that the behavior of powdered material is analogous to that of particle material to some extent, which is affected mainly by contact and dry frictions [4]. As a highly dissipative system, the motion procedure exhibits various physical states. The behavior of tiny dust is analogous to smoke when affected by air friction. Thus we choose the density field to represent the dust cloud. Meanwhile, we introduce moisture to particles' properties and use a geometry-based model to handle the viscous liquid phase, which is generated by the gathered particles. And we can imitate different viscosity by controlling the yield conditions. Our hybrid model is built upon the flexible and effective intertwinement of the Lagrange particle system, and the Eulerian density field, wherein the distributions and transitions of the granular particles and liquid phase are handled at the geometry level. At the same time, the dynamics are tightly coupled at the physics level. The salient contributions of this paper can be summarized as follows.

- We advocate an Euler-Lagrange coupled approach to the realistic simulation of the natural mixtures of different-sized particles and smoke-like density field, enabling physics-meaningful detail enhancement via smooth transition among large particles, dust cloud, and tiny particles.
- We introduce a moisture transfer model to control the transition process between discrete granular particles and continuous liquid phases, which provides a flexible way to simulate more complex scenarios involving multi-scale materials.
- We develop a unified framework to model various kinds of multi-scale granular material behaviors by flexibly controlling the parameters and the corresponding yield conditions, which can simulate many intriguing fluid-like phenomena for graphics applications.

2 Related Works

Euler-Lagrange coupled models. For the simulations of multi-scale granular materials, mixing both particle approach and grid methods allows keeping the high-resolution details from particles while relying on a background grid can reduce the number of DoF (degrees of freedom) and computations of the system. Thus Euler-Lagrange coupled models such as FLIP/PIC/APIC [15], [16], [14], and MPM [17], [18], [19] play important roles. Foster et al. [20] first introduced PIC techniques to computer graphics with liquid simulation by solving the N-S equation on the grid and used the labeled particles to track the fluid elements. Enright et al. [21] proposed a particle level set (PLS) method, adding particles on both sides of the liquid surface, compensate for the lack of details when the lower-level set function identifies the surface. Zhu and Bridson [4] popularized the widely-used linear combination of FLIP and PIC, and Later Bridson et al. [22] developed a number of extensions, including improved treatment of boundary conditions in irregular domains and coupling with rigid bodies, viscosity treatment [23], discontinuous-Galerkin-based adaptivity [24], multiphase flow [25] and higher-order accuracy [26]. Then, Cornelis et al. [27] coupled high-resolution FLIP based on the implicit incompressible SPH model [28]. Gerszewski et al. [29] used mass-full FLIP with a unilateral incompressibility constraint to resolve large-scale splashing liquids. Chentanez et al. [30] coupled the 3D Eulerian grid, particle, and height field method to simulate large-scale fluid scenes, which simultaneously met the real-time interactivity of fluid detail retention and simulation. Hu et al. [19] introduced a moving least squares model, which runs two times faster than existing MPM simulations. Daviet et al. [6] successfully used APIC to achieve continuous granular material simulation, and the simulation effect is realistic. Then, Frost et al. [31] created a proprietary APIC fluid solver for various water simulations.

Compared to popular FLIP/PIC models, APIC can produce more stable movement while simultaneously resolving more energetic details than the classical FLIP/PIC methods. Considering these advantages of APIC and our simulating target's complexity, we adopt APIC as the basic simulation framework.

Multi-scale materials simulation. Since multi-scale materials always have complex compositions and diverse behaviors, many researchers treated them as granular materials. Bell et al. [32] proposed a method for simulating granular materials based on Lagrangian particle representation. Hybrid methods were first applied to granular materials in computer graphics by Zhu and Bridson [4], and they used a unified FLIP/PIC framework to handle the sand-like behaviors. Stomakhin et al. [17] chose to let the particles carry more properties (such as mass and temperature) and used the MPM method to couple the particles with the grid for snow simulation, and extended this method to simulate melting and freezing [33] phenomena. Then Ram et al. [18] introduced a MPM-based model into the APIC method [5] to simulate viscoelastic fluids, foams, and sponges, using similar implicit time step of [33] and also achieved good performances. Klàr et al. [7] used the Drucker-Prager model to represent plasticity by factoring deformation gradient into both elastic and plastic parts, which recreates many convincing visual phenomena involving sand. After that, Tampubolon et al. [11] proposed a multi-species model for simulating the interaction of gravity-driven landslides and debris flows with porous sand materials and water, and realized the realistic modeling of sand behavior with different humidity. Fei et al. [34] developed a multi-scale model to simulate liquid-hair interactions, which uses the PIC model for liquid solving and a discrete rod model for hair simulation, achieving charming visual results. Gao et al. [35] proposed a hybrid semi-implicit MPM method to simulate particle deposition, using two MPM background grids to handle fluid and sediment two-way coupling. Yue et al. [36] proposed a hybrid method for granular material modeling that dynamically divides particles as discrete and continuum parts and achieves realistic performances. In summary, simulations of powdered/granular materials and their interactions have already achieved great success. Most of the previous works simulated the multi-scale materials with a single component, ignoring their possibly complex compositions and motion behaviors. However, these still have some works focus on the various sizes of particles when modeling granular materials. Liu et al. [37] proposed a physics-based approach to simulate sandstorms,

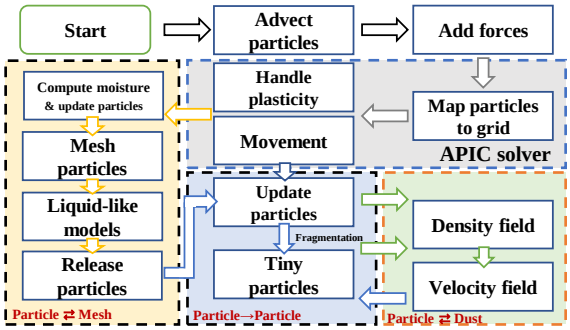

Fig. 1. The framework of our model.

using a relatively stable incompressible multi-fluid model to simulate the motion of air, sand, and dust particles. Then, they simulated a two-fluid phenomenon consisting of gas flow (wind field) and dust particle flow in a unified framework based on a Reynolds averaged two-fluid model (RATFM) [38]. Wang et al. [39] proposed a physics-based model that can synthesize various modes of sand. Yang et al. [40] proposed a hybrid model to simulate the behavior of multi-scale droplets and mist spray mixtures. Gao et al. [14] introduced a hybrid framework for powdered materials modeling, which involves dust cloud, dust particles, and granular particles.

Inspired by the previous works, we aim to realize a grid-particle-density field framework that simultaneously simulates individual particles, dust cloud, viscous liquid, their natural mixture, and transformations, accommodating physical meaning and ensuring the high-effective at the same time.

3 Method Overview

Our hybrid model for multi-scale granular materials consists of three tightly integrated phases: particle-based granular materials, a density-field-based dust cloud, and a surface-based liquid phase. All the materials are modeled by the APIC method. As to granular material simulation, the major difference distinguishing particles from the continuous liquid is the contact manner and dry friction [4]. Details are explained in section 4.1. Meanwhile, we employ a density-field-based solver to simulate dust cloud generated by atomization of granular particles (in Section 4.2) and surface mesh geometry for viscous liquid modeling (in Section 4.3).

3.1 Phase Transition Framework

To model the interaction and transition processes among different materials in computer graphics, we simplify the complex physical phenomenon into two essential steps: the transition between particles and density field and the transition between particles and liquid phase. As indicated in Fig. 2, the transition between dust cloud and tiny dust particles is bilateral. For sand particles, breaking into dust particles with smaller diameter occurs at the positions where the movements and collisions are violent, or the contact with air is so drastic that the particles split into dust cloud. This process will be described in Section 5.1. As for dust cloud, once the density reaches a threshold or the movement becomes stagnant, dust suspended in the air gathers together into tiny dust particles (in Section 5.2). For the transition between liquid and particles, we introduce a moisture property to control when surface tracking mesh should be generated for the liquid phase. The moisture controls the separated particles transforming back to individual granular particles (in Section 5.3).

3.2 APIC Model

Our hybrid model builds upon on the APIC method [5], [15], [16], we employ this fluid solver for granular and tiny dust particles. Of which, dynamic steps are done on particles, and dynamic steps are tackled on the grid. Fluid dynamics is based on Navier-Stokes (N-S) equations, which conserve conservation of mass and momentum:

$$\nabla \cdot \mathbf{u} = 0, \tag{1}$$

$$\rho(\frac{\partial \mathbf{u}}{\partial t} + \mathbf{u} \cdot \nabla \mathbf{u}) = -\nabla p + \mu \nabla^2 \mathbf{u} + \mathbf{f}, \tag{2}$$

where ρ represents the density, $\mathbf{u}$ represents particle velocity, p represents the pressure, and $\mathbf{f}$ represents the external force.Staggered grid has been used to transfer properties:

$$m_a^n = \sum_p m_p \omega_{ap}^n, \tag{3}$$

$$m_a^n \mathbf{u}_a^n = \sum_p m_p \omega_{aip}^n (\mathbf{e}_a^T \mathbf{u}_p^n + (\mathbf{c}_{ap}^n)^T (\mathbf{x}_a - \mathbf{x}_p^n)), \tag{4}$$

where subscript a denotes x, y or z directions, subscript p and i represents particle p and grid node i, and $\mathbf{e}_a$ represents the unit vector in a direction. The weights are $\omega_{ap}^n = N(\mathbf{x}_a - \mathbf{x}_p^n)$, $N(\mathbf{x})$ is the common trilinear interpolation kernel, and $\mathbf{x}_a$ is the location of a MAC face associated with direction a. m_a^n and $\mathbf{u}_a^n$ are the mass and velocity component, and $\mathbf{c}_{ap}^n$ is the affine vector per axis. When interpolating back, we transfer from grids to particles by

$$\mathbf{u}_p^{n+1} = \sum_{a,i} \omega_{aip}^n \tilde{\mathbf{u}}_{ai}^{n+1} \mathbf{e}_a, \tag{5}$$

and

$$\mathbf{c}_{pa}^{n+1} = \sum_i \nabla \omega_{aip}^n \tilde{\mathbf{u}}_{ai}^{n+1}, \tag{6}$$

where particles are endowed with mass $\mathbf{m}_p$, position $\mathbf{x}_p$, velocity $\mathbf{u}_p$ and three vectors $\mathbf{c}_{pa}$ represent the affine states. Relatively, properties conserved on grid are mass $\mathbf{m}_{ai}$(scalar), position $\mathbf{x}_{ai}$ and velocity $\mathbf{u}_{ai}$.

All the materials, including sand and liquid, are treated as liquid particles at first. The additional yield condition will be performed to simulate granular particles' gathering/separating behaviors (Section 4.1). As most PIC/FLIP-based models do, trilinear interpolation is used for the transitions from particle to grid. Although trilinear interpolation may produce discontinuous forces [7], we do not find it problematic in practice. Compared with the FLIP/PIC model, the most crucial improvement of APIC is the 3D affine velocity fields of the three vectors stored on every particle. This improvement enables the APIC method to

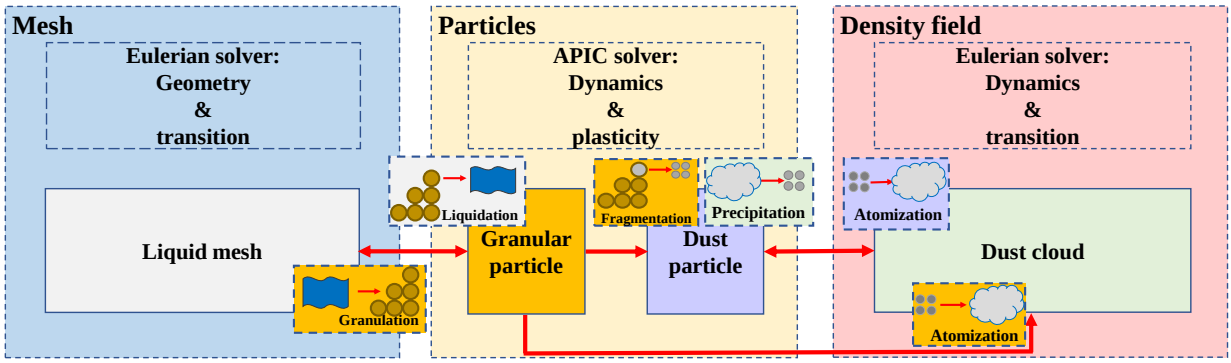

Fig. 2. The relationship of phase transitions among granular particles, dust cloud/particles, and liquid mesh.

avoid the PIC model's dissipation and unstable behaviors in the FLIP model. Thus, the exact conservation of angular momentum across the transfers between particles and grid is available. That benefits our simulation a lot since the tangential and rotational motions are pretty essential to represent the granular particles' behaviors.

4 Multi-scale Materials Modeling of Granular Particles, Liquid, and Dust Cloud

In this section, we will explain the three modeling parts of our proposed framework 2, include Lagrangian-particle-based particles modeling, density-field-based dust cloud modeling, and Eulerian-grid-based liquid modeling.

4.1 Yield Condition for Granular Particles Modeling

Drucker-Prager is a common yield criterion for granular materials modeling [41], [42], [6]. We use APIC [5] as our basic model for the dynamics simulation of all materials. And our constitutive model is an incompressible flow with Drucker-Prager plasticity [4]. It ignores elastic deformation and treats the granular domain as *rigid-plastic* flow. Compared to some existing granular models [7], [19], [36], our model is easy to be combined with the APIC method and is flexible to switch the simulations for different scales or phases involving liquid and granular particles. It characterizes simple strategies and a high performance-price ratio with satisfying graphics applications in practice.

To simulate sand-like behaviors, an external operating part will be added right after the grid's projection step. First, we evaluate the strain rate tensor $\mathbf{D}$ in each grid cell with standard central differences by

$$\mathbf{D} = (\nabla \mathbf{u} + \nabla \mathbf{u}^T)/2, \tag{7}$$

where $\nabla \mathbf{u}$ is the gradient of velocity field, and $\nabla \mathbf{u}^T$ represents its transposition.

Then we calculate the frictional stress by

$$\sigma_{\mathbf{f}} = -sin\Phi p \frac{\mathbf{D}}{\sqrt{1/3}\,|\mathbf{D}|_F}, \tag{8}$$

where Φ is the friction angle, p is the pressure computed in the projection step, and $|\mathbf{D}|_F$ is the Frobenius norm of $\mathbf{D}$. $\sigma_{\mathbf{f}}$ represents the maximum frictional force under current normal pressure to resist relative movement between grid cells. As for a static granular particle, the static stress $\sigma_{\mathbf{r}}$ is related to its density ρ:

$$\sigma_{\mathbf{r}} = -\frac{\rho \mathbf{D} \triangle \mathbf{x}^2}{\triangle t}, \tag{9}$$

where $\triangle \mathbf{x}$ is the cell size of grid solver, and $\triangle t$ represents the time step. This equation means the minimum stress required for rigidifying particles between two grid cells. Thus, against the Drucker-Prager criteria, we can determine the yield condition for each cell by:

$$|\sigma_r|_F < |\sigma_f|_F + c, \tag{10}$$

where $|\cdot|_F$ amounts to the Frobenius norm, and c represents the cohesion coefficient, this is to add some cohesion and avoid slippage before yielding. Including a bit of cohesion will improve the results for supposedly cohesion-less materials like sand. That is, if the resulting σ_r satisfies the yield condition, it will be marked as a rigid grid cell, and we store the static stress is σ_r. Otherwise, we store the sliding frictional stress σ_f.

Then the two regions are treated respectively [4]: for solidification cells, we find all connected groups of these cells, and project the velocity field in each separate group to the space of solidification cells' motions

$$\mathbf{u}(\mathbf{x}) = \bar{\mathbf{u}} + (\mathbf{x} - \bar{\mathbf{x}}) \times \bar{\omega}, \tag{11}$$

where $\bar{\mathbf{x}}$ represents the center of the connected group, $\bar{\mathbf{v}}$ represents the average velocity, and $\bar{\omega}$ is the average angular velocity. As for all the non-solidification cells, we update velocity by

$$\mathbf{u} = \mathbf{u} + \frac{\triangle t}{\rho} \nabla \cdot \sigma_f. \tag{12}$$

Moreover, we also change the general boundary condition to a frictional boundary condition. With the velocity adjustment using the yield condition, we can turn a standard APIC fluid solver into a simplified continuum solver for granular particles modeling.

4.2 Density Field for Dust Cloud Modeling

As for the modeling of the density-based dust cloud, we employ the Eulerian-based representation. When the velocity satisfies the generation criteria, we compute the density

Fig. 3. Illustration of different components of multi-scale materials. (a) shows granular particles, dust particles, dust cloud existing in one scene. (b) consider the moisture property and liquid mesh, there are liquid, granular particles, dust particles, and dust cloud coexisting.

field. When the dust cloud is generated, we delete the same amount of particles and emit dust cloud at the same position simultaneously. Conservation condition is ensured through the same initial value of density and velocity field. The velocity of dust cloud density field $\mathbf{u}_d$ is decided by

$$\rho(\frac{\partial \mathbf{u}_d}{\partial t} + \mathbf{u}_d \cdot \nabla \mathbf{u}_d) = -\nabla p + \mathbf{f}, \tag{13}$$

where $\mathbf{f}$ is additional force and p is the pressure. In our model, we replace this additional force with air resistance as a user-defined force. Then, we govern the density field by

$$\frac{\partial \rho}{\partial t} + \mathbf{u}_d \cdot \nabla \rho = \lambda \nabla^2 \rho - d\rho + S, \tag{14}$$

where λ is the diffusion coefficient, d represents the dissipation coefficient, and S contains the surrounding area in dust cloud source.

Note that when we use the Eulerian method to simulate smoke-like material since the material component usually has relatively little mass and volume, which is easily affected by the air buoyancy. The dust cloud will settle into small tiny particles under gravity force in a long enough period. Meanwhile, we set the dissipation coefficient d to $\mathbf{0}$ in all our simulation scenes.

4.3 Geometric Mesh for Liquid Modeling

At the computational level, the dynamics computation of the liquid phase is the same as granular particles. We can change the parameters of the yield condition to imitate different liquid phases with different viscosities. However, at the geometrical level, the most significant difference between liquid and powdered material is that liquid always has a continuous surface while powdered material consists of separated particles. In the real world, more wet the granular particles are, more likely they will behave like a viscous liquid, such as mud water. On the contrary, the dry granular particles always move like separated powders.

To simulate liquid phase, We use the level set procedure of [25] to set grid cells' markers, indicating whether it represents particles or density field. This information is necessary and used in different steps. Take an example, for boundary conditions settings we specifically perform frictional boundary conditions for the sand cells. We use an SDF function to track the surface of the liquid and the marching cube method [43] to reconstruct liquid surface mesh, distinguishing liquid from other particle-based materials. Only granular particles can turn into liquid particles contained in liquid mesh to reproduce the natural physical process. Dust particles and dust cloud are too small to generate a continuous liquid surface. That is to say, for dry materials, there are granular particles, tiny particles, and dust cloud coexisting simultaneously. For wet materials like mudslide, liquid phase, granular particles, will be mixed with dust particles and dust cloud in one scene. We introduce an additional moisture parameter to tackle the transformation between liquid mesh and particles. As shown in Fig. 3, moisture affects the morphology of multi-scale materials, the left figure shows the components of dry powdered materials, and the right figure illustrates the components of all the mixed materials, which considers moisture and liquid phase. The detailed transition process will be discussed in Section 5.4.

5 Transitions among Different Phases

This section will expand on our transition processes of particles-cloud and particles-liquid, focusing on the transition condition and material conservation. The transition from particles to the density field occurs only on the interface between particles and air or nearby positions. In other words, we need to judge if at least one air cell exists near a granular particle. However, if one granular particle inside satisfies the generation condition, it will not be transferred into the density field of dust cloud. Instead, it will be broken into smaller particles with a smaller diameter as tiny dust particles directly.

Note that for the APIC method, each particle represents not one but a clump of material. Thus one granular particle may break into several dust grains under the internal or external forces. This assumption can help better understand our transition procedure among granular particles, dust particles, and dust cloud.

5.1 Transition from Granular Particles to Dust Particles

If a granular particle meets the transition velocity but has no air cell neighbors, it will be broken into dust particles, and the velocity of dust particles is inherited from its father granular particle. The mass of generated dust particles is defined as:

$$m_{di} = \alpha \cdot m_i, \alpha \in [0, 0.5], \tag{15}$$

where m_{di} is the mass of dust particle, α is a parameter related to the velocity, the generated number of dust particles is $1/\alpha$ so the dust generation process can satisfy mass conservation. Since α is no greater than 0.5, it means two dust particles will be generated at least.

5.2 Transition from Particle Phase to Density Field

The essence of dust cloud generation is that a particle creates violent friction with the surrounding particles and has enough space (air cell neighbors) to diffuse. Because the two kinds of particles (granular and dust particles, which have air cell neighbors) produce dust cloud in the same manner, we name them *'particle/particles'* in this subsection and need not distinguish them. For the sake of modeling the transition from particle phase to density field, we simplify the transform conditions into two cases: particle has

relatively high speed to its neighbors or particle is in an absolute high-speed moving.

We calculate the relative velocity between one particle and its surrounding particles:

$$\mathbf{u}^{rel} = \mathbf{u} - \frac{\sum_{i \in S} m_i \mathbf{u}_i W(\mathbf{d}_i, \mathbf{h})}{\sum_{i \in S} m_i W(\mathbf{d}_i, \mathbf{h})}, \tag{16}$$

where $\mathbf{d_i}$ is the distance between the cell center and the particle, and $W(\mathbf{d}, \mathbf{h}) = max(0, 1 - \mathbf{d}^2/\mathbf{h}^2)$ is a smooth weighting function, details can be found in [40], [44]. Here we set $\mathbf{h} = \Delta \mathbf{x}/\sqrt{2}$ to compute the average values of nearby particles. Then we compare $\mathbf{u}^{rel}$ with the threshold $\mathbf{u}_{th}^{rel}$, once $\mathbf{u}^{rel}$ is larger than the artificial threshold, this particle will turn to be dust cloud. Meanwhile, we consider another situation when the particle's overall movement is intense, but the relative speed in this area may not large. Thus the overall activity may also violent enough to generate sufficient driving force to promote the transition. So we set an absolute threshold $\mathbf{u}_{th}^{max}$ to handle this situation. When the transition occurs, we select adjacent 8 cells near the position of the particles according to the diffusion coefficient, distribute the values proportionally to the density field of these cells with a trilinear interpolation function. The transition process is developed from the handling method for spray-droplet transition, and details can be found in Yang's work [40].

Collectively, the transition from particle phase to dust cloud has to satisfy two situations: the first one is that the particle should be close to the surface (e.g., the position is in contact with air). The second situation is that the difference between the velocity of the particle and its average velocity reaches the relative velocity threshold $\mathbf{u}_{th}^{rel}$, or its absolute velocity reaches the absolute velocity threshold $\mathbf{u}_{th}^{max}$. When only the second condition is satisfied, the granular particle will fragment to dust particles instead of dust cloud. Note that both large granular particles and tiny dust particles can generate the density field of dust cloud. The only difference between them is that large granular particles inside may transform into dust particles if it has no air cell neighbors, but the vice versa will not happen.

5.3 Transition from Dust Cloud to Dust Particles

In the real world, the flour will eventually fall to the ground, sandstorms without wind will also turn into dust piles. So we design a two-way transition framework to imitate this physical process of dust accumulation. Static dust cloud will generate dust particles. Wherein many tiny dust particles are clustered in a small area. We then compute the cell density:

$$\rho_c = \beta N \bar{\rho}, \tag{17}$$

where N is the number of neighbor cells equals 8 or 27, $\bar{\rho}$ is the average density of these N neighbor cells, and β is a coefficient used to control the expenditure of density field. The transition process occurs when one grid cell's density reaches a threshold ρ_{th}. Meanwhile, $\beta > \frac{1}{N}$ should be satisfied to avoid the repeated and meaningless transition within a single time step.Here we set $\beta = 1$, which facilitates mass conservation and dust particle generation. However, we need to consider this case that if the density reaches

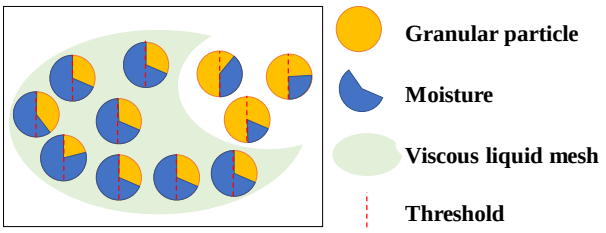

Fig. 4. Schematic diagram of surface mesh liquid and granular particles with different levels of moisture.

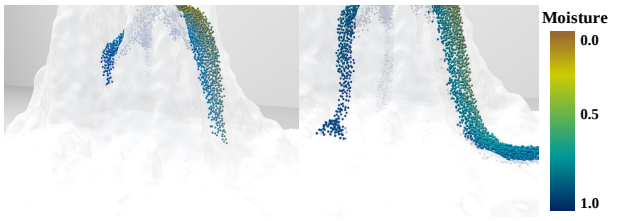

Fig. 5. Illustration of the moisture transfer process between granular particles and liquid phase. When the moisture of a particle reaches the threshold, it will be involved in the liquid mesh. When the moisture is less than the threshold, it will be released from the liquid mesh.

ρ_{th} and the dust cloud is still moving at high speed, the transition may not happen, such as sandstorm. Therefore, it is also necessary to set a minimum threshold $\mathbf{u}_{th}^{min}$. It means a dust particle will be generated only when the density is bigger than ρ_{th} and velocity is smaller than $\mathbf{u}_{th}^{min}$ at the same time. After dust particle is generated in a grid cell, we update the cloud density by

$$\rho_c = \rho_c - \beta N \bar{\rho}, \tag{18}$$

In another case, as the movement slows down, the velocity of dust cloud tends to be 0, but its density has not reached ρ_{th}. It means the diffused density field of the grid cell cannot be accumulated into dust particles. As a result, we consider the little dust cloud as discrete parts and ignore them. To explain this, powdered materials can hardly remain conservation in all quantities after movements to some extent, so it is reasonable to regard a small part of dust cloud as a discrete part that is dissipated.

5.4 Transitions between Granular Particles and Liquid Phase

Wet particles often flow like a viscous liquid, and the more water particles have, the more they behave like a liquid. To simulate the liquid-like phenomena of multi-scale granular material, we add the property of moisture to granular particles, and introduce an approximate model concerning the heat transfer model to simulate the changes of moisture when a large number of particles interact with each other.

The moisture of particles is initialized for each granular particle and will be mapped to the center of each APIC grid cell with a weight function, the exchange value among particles is:

$$M_g = \frac{\sum_{i \in S} M_i W(\mathbf{d}_i, \mathbf{h})}{\sum_{i \in S} W(\mathbf{d}_i, \mathbf{h})}, \tag{19}$$

where M_g, M_i are the moisture values of grid cell and particle p_i, respectively. S is the surrounding neighboring particles. To obtain the moisture field on grid, we discretize it along three directions:

$$\frac{M^{n+1}-M^n}{\Delta t}=\gamma(\frac{\partial^2 M^{n+1}}{\partial x^2}+\frac{\partial^2 M^{n+1}}{\partial y^2}+\frac{\partial^2 M^{n+1}}{\partial z^2}), \quad (20)$$

where M^n is the given moisture obtained in the last time step and M^{n+1} is the current one. Since moisture may diffuse to the air as evaporation, we correct the corresponding diffusivity by the parameter γ.

Our moisture conduction model is similar to the heat diffusion model [45]. One significant difference is that we do not need to consider the influence of mass on moisture. As shown in Fig. 4, after updating the change of moisture to granular particles, we determine whether the moisture of each particle is sufficient to be involved in the liquid mesh:

$$\begin{cases} P_g \rightarrow P_l, & M_p \geq M_{th} \\ P_g \leftarrow P_l, & M_p < M_{th}. \end{cases} \quad (21)$$

Here, P_g is a granular particle with moisture M_P, M_{th} is the threshold to control the change between granular particle and liquid particle. P_l is a liquid particle that should be involved in the geometric liquid mesh S_l. As shown in Fig. 5, we display the process of granular particles' moisture transfer.

6 Implementation Details

In this section, we itemize all the procedures of our method and supplement our implementation details.

6.1 Algorithm Integration

The whole procedure of our model within each time step is shown in Algorithm 1. This algorithm includes all the main calculations and measures for the hybrid interactions and transitions among granular particles, dust cloud, dust particles, and liquid mesh. Flexibly, we can enable or disable some phenomena through the program switch, as illustrated in the following algorithm.

6.2 Boundary Condition

We adopt the frictional boundary condition to tackle the friction between powdered material and boundaries. Since our boundaries and interacted objects are static solids, we use the simple wall boundaries [14] as the boundary condition:

$$\mathbf{u}_T = max(0, 1-\frac{\mu\,|\mathbf{u}\cdot n|}{|\mathbf{u}_T|})\mathbf{u}_T, \quad (22)$$

where $\mathbf{u}_T$ is the tangential velocity, μ is the friction coefficient between powdered material and boundaries (walls, solid objects), $|\mathbf{u}\cdot n|$ is the normal velocity, and $\mathbf{u}_T$ is the tangential velocity. Through this formula, we can realize external friction treatment. And for the positions where the normal velocity is much greater than the tangential velocity, the tangential velocity will be reduced to zero instead of inverse velocity in the opposite direction.

Algorithm 1 Implementation of our integrated framework for multi-scale granular material

Advect particles
Enforce external forces to each particle p
Map every particle p's properties to grid g
Solve the divergence-free velocity and incompressibility
if grid cell g contains granular/dust particles **then**
    Compute absolute velocity $\mathbf{u}^{rel}$ and relative velocity $\mathbf{u}$ using Eq. 16
    if ($|\mathbf{u}^{rel}| > |\mathbf{u}_{th}^{rel}|$ & air cell neighbor exists) || ($|\mathbf{u}| > |\mathbf{u}_{th}^{max}|$) **then**
        Generate density field for dust cloud
    if ($|\mathbf{u}^{rel}| > |\mathbf{u}_{th}^{rel}|$ & no air cell neighbors) **then**
        Generate dust particles using Eq. 15
    Calculate Yielding Condition (Sec. 4.1)
    if g is in solidification cells using Eq. 10 **then**
        Update unified velocity using Eq. 11
    else
        Update separate velocity using Eq. 12
    Apply frictional boundary condition (Sec. 6.2)
    Compute moisture transfer using Eq. 20
    Update moisture using Eq. 21
if grid cell g contains density field **then**
    Advect density field and velocity field
    if (Cell density $\geq \rho_{th}$ & cell velocity $< |\mathbf{u}_{th}^{min}|$) **then**
        Generate dust particles and update density using Eq. 18
Map grid g's properties back to particle p
if particle p 's moisture reaches threshold $M_p > M_{th}$ **then**
    p is a liquid particle ($p \in P_l$)
else
    p is granular particle ($p \in P_g$)

7 Experimental Results and Comparisons

7.1 Experimental Settings and Implementation Details

Our hybrid model has been implemented with C++ and CUDA, while all experiments are run on a PC of 3.40GHz Intel Core i7 CPU and Geforce GTX1080 GPU. All the results are rendered by *Blender (https://www.blender.org)*. We design several scenarios to verify the effect and reality of the simulation model. Table 1 shows several performances and key parameters setting of our experiments.

7.2 Scenes Design and Applications

Sand pouring and explosion. As shown in Fig. 6, powdered particles pour and interact with a static solid model hanging in the air. The density field and tiny particles are generated from large granular particles. Fig. 7 shows the powdered particles exploding in the center of the scene. When the explosion happens, the particles fly along in all directions, and the dust cloud has been quickly generated. Since there is no external force driving, dust cloud soon transfers to tiny dust particles, and all particles drop down under gravity.

Sandstorms phenomenon. In a closed scene, driven by an artificial tornado the sand particles are rolled into the air under a spiral wind field like a sandstorm. As the movement

TABLE 1
Parameters setting and time performances of the experimental results.

Scenes	Resolutions	Particles	Time/Frame	$\mathbf{u}_{th}^{max}$	$\mathbf{u}_{p}^{rel}$	ρ_{th}	$\mathbf{u}_{th}^{min}$
Interaction 1 (Fig. 13)	96x96x96	400k	146.54ms	1.0	0.2	0.1	0.03
Interaction 2(Fig. 6)	96x96x64	80k	61.32ms	2.0	0.2	0.02	0.03
Explosion (Fig. 7)	96x96x96	150k	67.24ms	4.0	0.5	0.05	0.05
Sandstorm (Fig. 8)	64x64x64	400k	50.80ms	3.5	0.5	0.03	0.05
Horse 1 (Fig. 9) (a)	64x64x64	200k	40.59ms	1.0	0.2	0.05	0.05
Horse 2 (Fig. 9) (b)	64x64x64	200k	26.54ms	-	-	-	-
Horse 3 (Fig. 9) (c)	64x64x64	200k	3.17ms	-	-	-	-
Mudslide (Fig. 10)	128x128x128	300k	258.02ms	2.0	0.2	0.1	0.01
Concrete mixture (Fig. 11)	96x96x96	120k	62.21ms	2.0	0.2	0.08	0.02

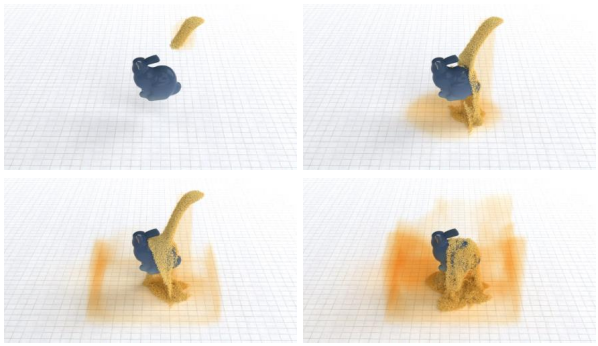

Fig. 6. Pouring sand onto a solid model hanging in the air. Sand particles interact with solid to generate dust cloud and dust particles.

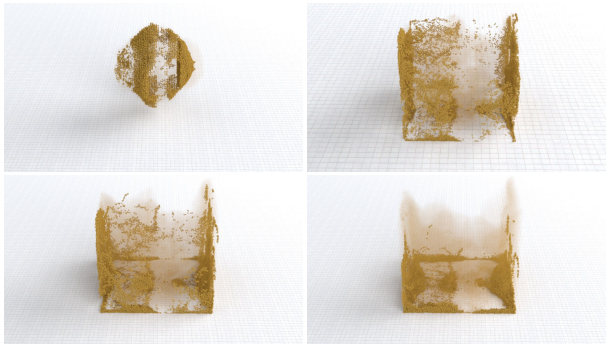

Fig. 7. A cloud of grained sand-like materials explode in a sandbox.

becomes more intense, a dust cloud is generated and moves along with the granular particles. When the simulation progresses to a certain time point, the wind disappears, and the powdered material hits the wall, then slides back to the ground. Dust cloud gradually deposits as tiny dust particles and drops down to the ground.

Different yield conditions. We can control the different stacking effects of granular materials through the yield conditions and realize various phenomena with different friction forces and different viscosities. As shown in Fig. 9, horse models fall on the ground under the same gravity. Fig. 9 (a) illustrates granular sands' behavior of transformations with different scales of particles and dust cloud. Fig. 9 (b) only has granular particles. We can imitate viscous

Fig. 8. Powdered material has been rolled into the air due to the spiral wind. Dust cloud, and dust particles are generated as the particles rotate.

liquid performance by canceling the particles transformations and dust generation by yield condition. Fig. 9 (c) is a complete water phenomenon without the constraint of yield condition and particle transformation process. Our method can hardly strictly meet the physical laws, but we can easily and quickly simulate various discontinuous material phenomena by controlling parameters. Please note that in Fig. 9 (b) and (c), we cancel the generating process of granular particles to liquid mesh for clear contrasts.

Mudslides and concrete mixture. As shown in Fig. 11 and Fig. 10, granular particles with the initialized moisture flow down, moisture transfers among particles, and a collection of humid granular particles form the surface mesh as liquid phase. In contrast, other granular particles may form dust particles or density field. In these two experiments, M_{th} is 0.4, which means when a granular particle's moisture is larger than 0.4, it will turn to be a liquid particle and be involved in the liquid phase.

7.3 Comparisons and Discussions

This scene shows throwing progress with different parameters for dust cloud generation (Fig. 12). A pile of powdered particles is thrown from the center with an initial velocity and different transfer threshold parameters. Detailed parameters setting has been illustrated in Table 2. There are three behaviors of different degrees for dust cloud generation, with an extremely high threshold $\mathbf{u}_{thres}^{max} = 100$,

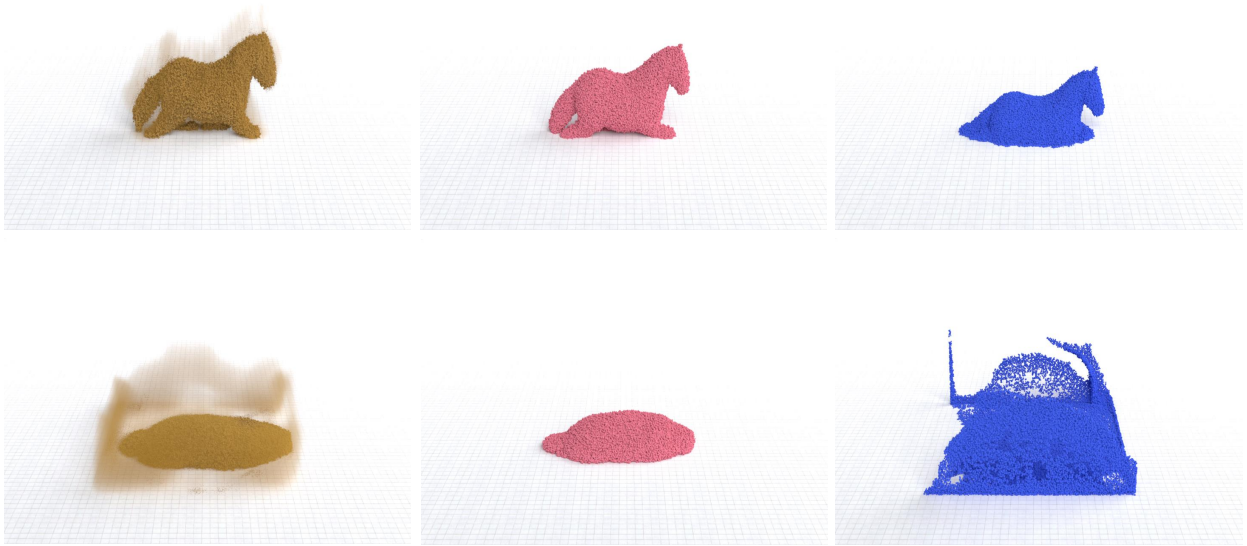

(a) (b) (c)

Fig. 9. Different multi-scale granular phenomena. (a) shows the behavior of powdered material. (b) forbids the transitions from granular particles to dust particles and dust cloud, thus can imitate viscous liquid by controlling the yield condition. (c) cancels the yield constraint and all transition procedures, which behaves like a traditional APIC water dynamic scene.

Fig. 10. Mudslides fall along the mountain model. The mud-water mixture flows down from the mountain model, containing viscous liquid, different sizes of particles, and dust cloud.

TABLE 2
Parameters setting for the comparison of dust cloud generations.

Scene	$\mathbf{u}_{th}^{max}$	$\mathbf{u}_{th}^{rel}$	ρ_{th}	$\mathbf{u}_{th}^{min}$
Fig. 12 (b)	100	–	–	–
Fig. 12 (c)	4.0	0.5	0.03	0.03
Fig. 12 (d)	1.0	0.2	0.03	0.03

particles will not transfer to dust, and we can flexibly control the transfer degree depends on different applications.

Fig.13 illustrates the results of our hybrid powdered materials model solved by different solvers. As powdered materials drop-down under gravity force, an object moves forward and back quite fast to hit the particles. It can be seen from these three scenarios that, benefit from APIC, the angular momentum is conserved during simulation, leading to better rotating and floating effects of powdered materials.

Fig. 14 shows a scenario of interaction between powdered material and solid model. Fig. 14 (a) shows all the powdered materials of granular particles, dust cloud, and dust particles. Fig. 14 (b) has no dust cloud, and Fig. 14 (c) only uses the traditional one scale of the particle, which has no transitions of both dust cloud and particles. It can be obviously seen from Fig. 14, with our complete transition process, we can imitate more realistic details.

Fig. 15 displays the comparisons of mudslide phenomenon. Fig. 15 (a) shows our complete framework with a surface mesh of viscous liquid, granular and dust particles, and dust cloud interacts and transforms in one scene. Fig. 15 (b) has no viscous liquid and only includes particle and density field. Fig. 15 (c) cancels the transformation process between particles and dust cloud, and forbids the liquid mesh model. By comparing these three scenes, it can be seen that for the simulations such as mudslide, our mesh-particle-density field hybrid model can get a better and more realistic visual effect.

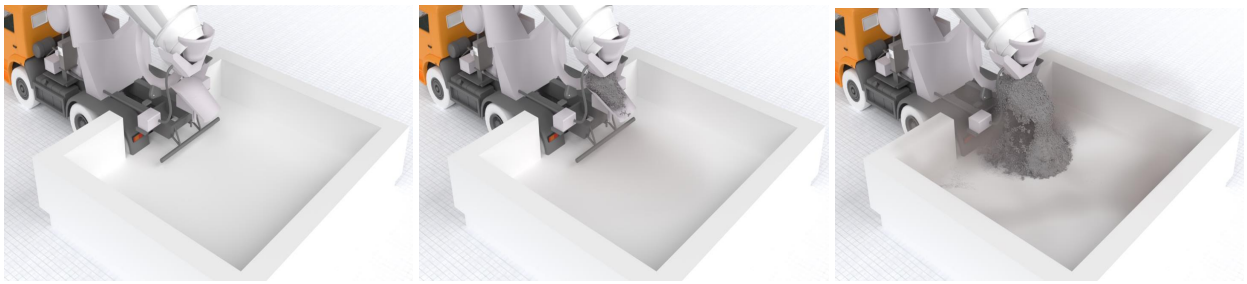

Fig. 11. A concrete truck pours the concrete mixture into the pool. The concrete mixture are flowing from the truck and spreading out at the pool bottom.

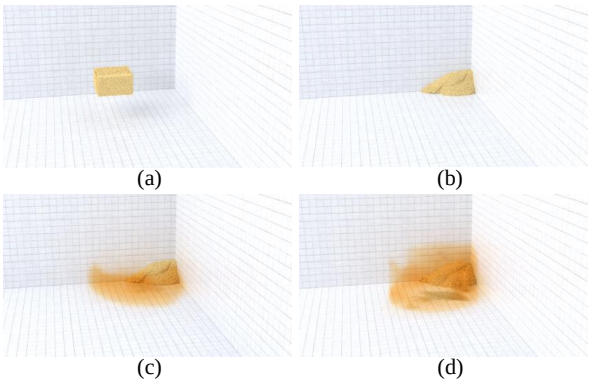

Fig. 12. Throwing sand to a corner with different thresholds. (a) is the initial state of this scene. (b) has no transition from particles to dust cloud. (c) shows a part of sand particles transforming to density. (d) shows a lot of dust cloud generated from sand particles.

7.4 Limitations and Discussions

There are still some limitations. The presented moisture property and viscous liquid transition process are based on physical principles, which provide meaningful theories and convincing visual results for the dynamic transformations among different materials. However, our granular particles perform plasticity and hardening as an additional step inserted into the APIC algorithm. Compared to some works concentrating on single granular materials simulation such as [7], our granular model may be insufficient to simulate such a wide range of sand phenomena. Nevertheless, we mainly focus on the multi-scale material modeling and their scale/phase transitions. The simplification does not affect the experimental results and has higher efficiency.

8 Conclusion

This paper articulate a flexible and simplified approach to the high-quality animation of the challenging natural phenomena involving multi-scale granular materials that span various ranges of particles from granular/dust material to liquid material and even dust cloud. Through the coupled Euler-Lagrange computational framework, materials of different states can be simulated simultaneously and can flexibly transit to each other. Our new approach affords various discontinuous fluid-like behaviors. As a result, we can produce vivid visual effects for powdered materials, granular materials, and viscous liquid in a critical state, which collectively enhance the modeling and animation capability involving powdered materials.

Our multi-scale method can be easily combined with other improved PIC models to obtain some of the benefits of both. With the advent of some enhanced methods such as polynomial-PIC [46] that has low dissipation, it will be a valuable attempt to combine our multi-scale material model with the aforementioned work towards better improvements. On the other hand, we are still using manual adjustment for the threshold setting relevant to the different materials and their transformations. In the future, building a relationship between moisture and yield condition is an interesting task, which will enable us to handle the cohesion or other physical properties by way of different moisture values..

Acknowledgments

This research is supported in part by Beijing Natural Science Foundation (No. 4214066), Beijing Advanced Innovation Center for Biomedical Engineering (ZF138G1714), National Natural Science Foundation of China (NO. 62002010), National Science Foundation of USA (NO. IIS-1715985 and IIS-1812606), CAMS Innovation Fund for Medical Sciences (CIFMS) (2019-I2M-5-016). We would like to thank the anonymous reviewers for paying time to raise constructive critiques to us.

References

[1] X. Yan, Y.-T. Jiang, C.-F. Li, R. R. Martin, S.-M. Hu, Multiphase SPH simulation for interactive fluids and solids, ACM Transactions on Graphics (TOG) 35 (4) (2016) 79:1–79:11.
[2] Y. Gao, Z. Zheng, J. Li, S. Li, H. Qin, Dynamic particle partitioning SPH model for high-speed fluids simulation, Graphical Models 109 (2020) 101061:1–101061:13.
[3] M. Macklin, M. Müller, N. Chentanez, T.-Y. Kim, Unified particle physics for real-time applications, ACM Transactions on Graphics (TOG) 33 (4) (2014) 153:1–153:12.
[4] Y. Zhu, R. Bridson, Animating sand as a fluid, ACM Transactions on Graphics (TOG) 24 (3) (2005) 965–972.
[5] C. Jiang, C. Schroeder, A. Selle, J. Teran, A. Stomakhin, The affine particle-in-cell method, ACM Transactions on Graphics (TOG) 34 (4) (2015) 51:1–51:10.
[6] G. Daviet, F. Bertails-Descoubes, A semi-implicit material point method for the continuum simulation of granular materials, ACM Transactions on Graphics (TOG) 35 (4) (2016) 102:1–102:13.
[7] G. Klár, T. Gast, A. Pradhana, C. Fu, C. Schroeder, C. Jiang, J. Teran, Drucker-prager elastoplasticity for sand animation, ACM Transactions on Graphics (TOG) 35 (4) (2016) 103:1–103:12.

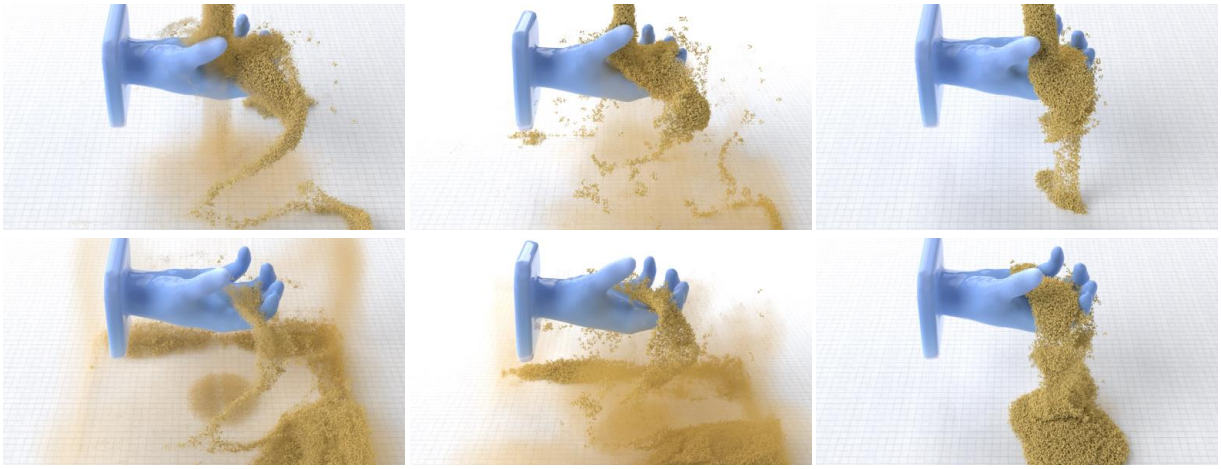

(a) (b) (c)

Fig. 13. Comparisons of different solvers with our hybrid model at the same frame. A moving object hits the following powdered materials with different dynamic solvers. (a) shows the APIC solver we used for all our experiments. (b) displays the FLIP solver, which makes particles and dust cloud violently scattered. (c) shows the result solved by PIC solver, which is too smooth to make the particle move very gently.

(a) (b) (c)

Fig. 14. Comparisons of our hybrid model for dry materials. (a) shows a powdered material simulation with granular particles, dust cloud, and dust particles. (b) displays powdered material simulation with different scales of particles. (c) shows granular materials simulation with a single scale of particles.

[8] X. Wang, M. Li, Y. Fang, X. Zhang, M. Gao, M. Tang, D. M. Kaufman, C. Jiang, Hierarchical optimization time integration for CFL-rate MPM stepping, ACM Transactions on Graphics (TOG) 39 (3) (2020) 1–16.

[9] C. Braley, A. Sandu, Fluid simulation for computer graphics: A tutorial in grid based and particle based methods, Virginia Tech, Blacksburg, 2009.

[10] J. Zhao, Y. Chen, H. Zhang, H. Xia, Z. Wang, Q. Peng, Physically based modeling and animation of landslides with MPM, The Visual Computer 35 (9) (2019) 1223–1235.

[11] A. P. Tampubolon, T. Gast, G. Klár, C. Fu, J. Teran, C. Jiang, K. Museth, Multi-species simulation of porous sand and water mixtures, ACM Transactions on Graphics (TOG) 36 (4) (2017) 105:1–105:11.

[12] T. Yang, J. Chang, M. C. Lin, R. R. Martin, J. J. Zhang, S.-M. Hu, A unified particle system framework for multi-phase, multi-material visual simulations, ACM Transactions on Graphics (TOG) 36 (6) (2017) 224:1–224:13.

[13] B. Andreotti, Y. Forterre, O. Pouliquen, Granular media: between fluid and solid, Cambridge University Press, 2013.

[14] Y. Gao, Y. Xu, S. Li, A. Hao, H. Qin, A hybrid method for powdered materials modeling, in: 25th ACM Symposium on Virtual Reality Software and Technology, 2019, pp. 1–10.

[15] C. Jiang, C. Schroeder, J. Teran, An angular momentum conserving affine-particle-in-cell method, Journal of Computational Physics 338 (2017) 137–164.

[16] O. Ding, T. Shinar, C. Schroeder, Affine particle in cell method for MAC grids and fluid simulation, Journal of Computational Physics 408 (109311) (2020) 1–29.

[17] A. Stomakhin, C. Schroeder, L. Chai, J. Teran, A. Selle, A material point method for snow simulation, ACM Transactions on Graphics (TOG) 32 (4) (2013) 102:1–102:9.

[18] D. Ram, T. Gast, C. Jiang, C. Schroeder, A. Stomakhin, J. Teran, P. Kavehpour, A material point method for viscoelastic fluids, foams and sponges, Proceedings of the 14th ACM SIGGRAPH/Eurographics Symposium on Computer Animation (2015) 157–163.

[19] Y. Hu, Y. Fang, Z. Ge, Z. Qu, Y. Zhu, A. Pradhana, C. Jiang, A moving least squares material point method with displacement discontinuity and two-way rigid body coupling 37 (4) (2018) 150:1–150:14.

[20] N. Foster, D. Metaxas, Realistic animation of liquids, Graphical models and image processing 58 (5) (1996) 471–483.

[21] D. Enright, R. Fedkiw, J. Ferziger, I. Mitchell, A hybrid particle level set method for improved interface capturing, Journal of Computational Physics 183 (1) (2002) 83–116.

[22] C. Batty, F. Bertails, R. Bridson, A fast variational framework for accurate solid-fluid coupling, ACM Transactions on Graphics (TOG) 26 (3) (2007) 100:1–100:8.

[23] C. Batty, R. Bridson, Accurate viscous free surfaces for buckling, coiling, and rotating liquids, Proceedings of the 2008 ACM SIGGRAPH/Eurographics Symposium on Computer Animation (2008) 219–228.

[24] E. Edwards, R. Bridson, Detailed water with coarse grids: combining surface meshes and adaptive discontinuous galerkin, ACM Transactions on Graphics (TOG) 33 (4) (2014) 136:1–136:9.

[25] L. Boyd, R. Bridson, MultiFLIP for energetic two-phase fluid simulation, ACM Transactions on Graphics (TOG) 31 (2) (2012) 16:1–16:12.

[26] E. Edwards, R. Bridson, A high-order accurate particle-in-cell

(a) (b) (c)

Fig. 15. Comparisons of our hybrid model for wet materials. In (a) we enable moisture property of granular particles and dust transformation, mudslide simulation with the viscous liquid, granular particles, dust cloud, and dust particles. There is no surface mesh of viscous liquid in (b). (c) has no dust cloud nor liquid transformation process.

method, International Journal for Numerical Methods in Engineering 90 (9) (2012) 1073–1088.

[27] J. Cornelis, M. Ihmsen, A. Peer, M. Teschner, IISPH-FLIP for incompressible fluids, Computer Graphics Forum 33 (2) (2014) 255–262.

[28] M. Ihmsen, J. Cornelis, B. Solenthaler, C. Horvath, M. Teschner, Implicit incompressible SPH, IEEE transactions on visualization and computer graphics 20 (3) (2013) 426–435.

[29] D. Gerszewski, A. W. Bargteil, Physics-based animation of large-scale splashing liquids., ACM Transactions on Graphics (TOG) 32 (6) (2013) 185:1–185:6.

[30] N. Chentanez, M. Müller, T.-Y. Kim, Coupling 3D eulerian, height-field and particle methods for interactive simulation of large scale liquid phenomena, IEEE transactions on visualization and computer graphics 21 (10) (2015) 1116–1128.

[31] B. Frost, A. Stomakhin, H. Narita, Moana: performing water, ACM SIGGRAPH 2017 Talks (2017) 30.

[32] N. Bell, Y. Yu, P. J. Mucha, Particle-based simulation of granular materials, in: Proceedings of the 2005 ACM SIGGRAPH/Eurographics Symposium on Computer Animation, ACM, 2005, pp. 77–86.

[33] A. Stomakhin, C. Schroeder, C. Jiang, L. Chai, J. Teran, A. Selle, Augmented MPM for phase-change and varied materials, ACM Transactions on Graphics (TOG) 33 (4) (2014) 138:1–138:11.

[34] Y. R. Fei, H. T. Maia, C. Batty, C. Zheng, E. Grinspun, A multi-scale model for simulating liquid-hair interactions, ACM Transactions on Graphics (TOG) 36 (4) (2017) 56:1–56:16.

[35] M. Gao, A. Pradhana, X. Han, Q. Guo, G. Kot, E. Sifakis, C. Jiang, Animating fluid sediment mixture in particle-laden flows, ACM Transactions on Graphics (TOG) 37 (4) (2018) 149:1–149:11.

[36] Y. Yue, B. Smith, P. Y. Chen, M. Chantharayukhonthorn, K. Kamrin, E. Grinspun, Hybrid grains: Adaptive coupling of discrete and continuum simulations of granular media, ACM Transactions on Graphics (TOG) 37 (6) (2018) 283:1–283:19.

[37] S. Liu, Z. Wang, Z. Gong, L. Huang, Q. Peng, Physically based animation of sandstorm, Computer Animation and Virtual Worlds 18 (4-5) (2007) 259–269.

[38] S. Liu, Z. Wang, G. Zheng, Q. Peng, Simulation of atmospheric binary mixtures based on two-fluid model, Graphical Models 70 (6) (2008) 117–124.

[39] N. Wang, B.-G. Hu, Real-time simulation of aeolian sand movement and sand ripple evolution: a method based on the physics of blown sand, Journal of Computer Science and Technology 27 (1) (2012) 135–146.

[40] L. Yang, S. Li, A. Hao, H. Qin, Hybrid particle-grid modeling for multi-scale droplet/spray simulation, Computer Graphics Forum 33 (7) (2014) 199–208.

[41] R. Narain, A. Golas, M. C. Lin, Free-flowing granular materials with two-way solid coupling 29 (6) (2010) 173:1–173:10.

[42] T. Lenaerts, P. Dutr, Mixing fluids and granular materials, Computer Graphics Forum 28 (2) (2010) 213–218.

[43] G. Akinci, M. Ihmsen, N. Akinci, M. Teschner, Parallel surface reconstruction for particle-based fluids, Computer Graphics Forum 31 (6) (2012) 1797–1809.

[44] R. T. Ryoichi Ando, Nils Thurey, Preserving fluid sheets with adaptively sampled anisotropic particles., IEEE Transactions on Visualization and Computer Graphics 18 (8) (2012) 1202–1214.

[45] Y. Gao, S. Li, L. Yang, H. Qin, A. Hao, An efficient heat-based model for solid-liquid-gas phase transition and dynamic interaction, Graphical Models 94 (2017) 14–24.

[46] C. Fu, Q. Guo, T. Gast, C. Jiang, J. Teran, A polynomial particle-in-cell method, ACM Transactions on Graphics (TOG) 36 (6) (2017) 222:1–222:12.

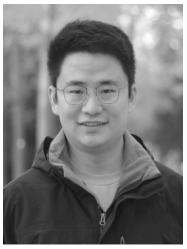

Yang Gao received the Ph.D. degree in computer science from Beihang University in 2019. He is currently an assistant professor at the State Key Laboratory of Virtual Reality Technology and Systems, Beihang University, Beijing. His research interests include computer graphics, VR/AR applications, physics-based modeling and simulation. In particular, he is focusing on fluid simulation.

Shuai Li received the Ph.D. degree in computer science from Beihang University. He is currently a professor at the State Key Laboratory of Virtual Reality Technology and Systems, Beihang University. His research interests include computer graphics, physics-based modeling and simulation, virtual surgery simulation, computer vision, and medical image processing.

Aimin Hao is a professor in Computer Science School and the Associate Director of State Key Laboratory of Virtual Reality Technology and Systems at Beihang University. He received his B.S., M.S., and Ph. D. in Computer Science at Beihang University. His research interests are in virtual reality, computer simulation, computer graphics, geometric modeling, image processing, and computer vision.

Hong Qin received his BS and MS degrees in computer science from Peking University, and his PhD degree in computer science from the University of Toronto. He is a professor of computer science in Department of Computer Science at Stony Brook University. His research interests include geometric and solid modeling, graphics, physics-based modeling and simulation, computer-aided geometric design, human computer interaction, visualization, and scientific computing. He is a senior member of the IEEE and the IEEE Computer Society.